Int J CARS (2017) 12:493–507
DOI 10.1007/s11548-016-1513-1

REVIEW ARTICLE

Breast ultrasound image segmentation: a survey

Qinghua Huang[1,2,3] · **Yaozhong Luo**[3] · **Qiangzhi Zhang**[3]

Received: 29 March 2016 / Accepted: 15 December 2016 / Published online: 9 January 2017

Abstract
Purpose Breast cancer is the most common form of cancer among women worldwide. Ultrasound imaging is one of the most frequently used diagnostic tools to detect and classify abnormalities of the breast. Recently, computer-aided diagnosis (CAD) systems using ultrasound images have been developed to help radiologists to increase diagnosis accuracy. However, accurate ultrasound image segmentation remains a challenging problem due to various ultrasound artifacts. In this paper, we investigate approaches developed for breast ultrasound (BUS) image segmentation.
Methods In this paper, we reviewed the literature on the segmentation of BUS images according to the techniques adopted, especially over the past 10 years. By dividing into seven classes (i.e., thresholding-based, clustering-based, watershed-based, graph-based, active contour model, Markov random field and neural network), we have introduced corresponding techniques and representative papers accordingly.
Results We have summarized and compared many techniques on BUS image segmentation and found that all these techniques have their own pros and cons. However, BUS image segmentation is still an open and challenging problem due to various ultrasound artifacts introduced in the process of imaging, including high speckle noise, low contrast, blurry boundaries, low signal-to-noise ratio and intensity inhomogeneity
Conclusions To the best of our knowledge, this is the first comprehensive review of the approaches developed for segmentation of BUS images. With most techniques involved, this paper will be useful and helpful for researchers working on segmentation of ultrasound images, and for BUS CAD system developers.

Keywords Breast cancer · Computer-aided diagnosis · Ultrasound · Segmentation

✉ Qinghua Huang
qhhuang@scut.edu.cn

[1] School of Electronics and Information, and Center for OPTical IMagery Analysis and Learning (OPTIMAL), Northwestern Polytechnical University, Xi'an 710072, Shaanxi, People's Republic of China

[2] College of Information Engineering, Shenzhen University, Shenzhen 518060, China

[3] School of Electronic and Information Engineering, South China University of Technology, Guangzhou 510641, China

Introduction

Breast cancer is the most common form of cancer among women worldwide and more than 8% women suffer this disease during their lifetime. Since the causes of breast cancer remain unknown, early detection is the key to reduce the death rate (40% or more) [1]. Early detection of breast cancer increases treatment options and patients' survivability [2]. However, early detection requires an accurate and reliable diagnosis which should also be able to distinguish benign and malignant tumors. A good detection approach should produce both low false positive (FP) rate and false negative (FN) rate.

Mammography used to be the most effective tool for early detection of breast cancer [1,3]; however, it has some restrictions. On a screening mammographic examination, noncancerous lesions can be misinterpreted as a cancer (FP value), while cancers may be missed (FN value). As a result, many unnecessary biopsy operations (65–85%) are implemented [4] and radiologists fail to detect 10–30% of breast cancers [5–7]. In addition, mammography can hardly detect

breast cancers in adolescent women with dense breasts, and the ionizing radiation of mammography can increase the health risk for the patients and radiologists. Therefore, ultrasound (US) imaging currently becomes an important alternative to mammography due to the following merits: no radiation, faster imaging, higher sensitivity and accuracy, and lower cost [8–12]. Also, it shows an increasing interest in the use of US images for breast cancer detection [13–16]. Statistics showed that more than one out of every four researches is using US images, and the proportion increases more and more quickly [17]. Studies have demonstrated that using US images can discriminate benign and malignant masses with a high accuracy [8,9], increase overall cancer detection by 17% [10], and reduce the number of unnecessary biopsies by 40% [18].

However, sonography is much more operator dependent than mammography, reading US images requires well-trained and experienced radiologists. Even well-trained experts may have a high inter-observer variation rate; therefore, the CAD has its potential to help radiologists in breast cancer detection and classification [19–21]. Recently, some CAD systems for breast cancer have been developed to reduce the expense and to improve the capability of radiologist. Generally, the breast cancer CAD system based on the US image involves the following four steps: image preprocessing, segmentation, feature extraction and selection, and classification. Among these four procedures, image segmentation which separates the lesion region from the background is the key to the subsequent processing and determines the quality of the final analysis. However, accurate US image segmentation remains a challenging problem [22] due to various US artifacts and noises, including high speckle noise [23], low signal-to-noise ratio, and intensity inhomogeneity [24]. In clinical practices, the segmentation task is generally performed by manual tracing, which is tedious, time-consuming, and skill and experience dependent. Hence, to improve the automation and robustness of CAD systems, reliable and automatic or semiautomatic segmentation methods are preferred to segment the region of interest (ROI) from the US image. Hence, this paper focuses on summarizing the segmentation techniques developed for the breast US (BUS) image (in a broad sense, for the breast B-mode US image).

To the best of our knowledge, there are only a few review literatures [22,25,26] focusing on or involving US image segmentation. In 2006, Noble and Boukerroui [22] focused on the techniques developed for segmentation of medical B-mode US images, and a review of articles by clinical application and a classification of methodology in terms of the use of prior information were presented. In 2010, a survey on the approaches used in the ultrasonic CAD system of breast cancer was presented according to the structure (i.e., preprocessing, segmentation, feature extraction and selection, and classification) of CAD system, by Cheng et al. [25]. In 2013, Jalalian et al. [26] presented a review on CAD of breast cancer in both mammography and US images. However, none of these is specifically focusing on segmentation of BUS images. As far as we know, this is the first comprehensive review of the approaches developed for segmentation of BUS images, and most techniques are included, especially those developed in the last decade. This paper will be useful for BUS CAD system developers and researchers.

The outline of this paper is as follows. The approaches developed for segmentation of BUS images classified by the adopted techniques are reviewed in "Segmentation techniques for BUS images" section, and the performance of segmentation methods are shown in "Performance evaluation of segmentation methods" section. Discussion and conclusions are drawn in "Discussion and conclusions" section.

Segmentation techniques for BUS images

Image segmentation is a process to partition a given digital image $\boldsymbol{I}$ into multiple nonoverlapping regions:

$$\cup I_i = I \quad \text{and} \quad I_i \cap I_j = \emptyset \quad i \neq j \tag{1}$$

The goal of segmentation is to simplify and/or change the representation of an image into something that is more meaningful and easier to analyze. Image segmentation is typically used to locate objects and boundaries (e.g., lines and curves) in images. More precisely, image segmentation is the process of assigning a label to every pixel in an image such that pixels with the same label share certain characteristics. The result of image segmentation is a set of segments that collectively cover the entire image, or a set of contours extracted from the image. Each of the pixels in a region is similar with respect to some characteristic or computed property, such as color, intensity, or texture. Adjacent regions are significantly different with respect to the same characteristic(s). When applied to a stack of images, typically in medical imaging, the resulting contours after image segmentation can be used to create 3D reconstructions with the help of interpolation algorithms such as marching cubes. In the breast cancer CAD system, the goal of segmentation is to segment the ROI, i.e., the lesion region, from the background. In this section, we present a review of approaches developed for BUS image segmentation by their adopted techniques.

Thresholding-based

Thresholding is one of the frequently used techniques for the monochrome image segmentation and was widely applied to segmenting BUS images [10,27–32]. As the simplest method of image segmentation, thresholding is based on a clip level (or a threshold value) to turn a grayscale image

Fig. 1 Thresholding in segmentation of BUS. *Left* The original BUS image; *middle* the segmentation result with the thresholding segmentation method; *right* the ROI after the morphological chain method [32]

into a binary image. The classic thresholding method is relatively simple and primitive, and may not perform well for the image with a unimodal histogram because it only considers gray level statistics, without taking spatial location information into account. Besides, there is a certain overlap ratio in the gray level distribution between the object and the background in some images. So a key step in thresholding methods is to select an appropriate threshold value (or values when multiple levels are selected). To this end, several popular methods are used in industry including the maximum entropy method, Otsu's method (maximum variance), and k-means clustering. A segmentation result with the thresholding method proposed in [32] is shown in Fig. 1.

During the period from 2001 to 2004, Horsch et al. [27,28,30] focused on the thresholding segmentation of BUS images and proposed improved algorithms involving the following steps: (1) preprocessing using cropping and median filtering, (2) multiplying the preprocessed image with a Gaussian constrain function, (3) determining the potential lesion margins through gray value thresholding, and (4) maximizing a utility function for each potential lesion margin obtained in (3). However, the center, width and height of the lesions need to be selected manually or semi-manually, which makes these algorithms not robust enough. In the experiment of [27], comparison consisted of a partially automatic and fully automatic version of the method with manual delineations on 400 cases, and four image-based features (shape, echogenity, margin, and posterior acoustic behavior) were computed to test the effectiveness at distinguishing malignant and benign tumors. Also, the advantages of different features were assessed using linear discriminant analysis in [28,30], where the best two features were found to be the shape and margin. Aiming at further automating the thresholding method, Drukker et al. [10] extended this work to include mass detection by first filtering the image with a radial gradient index filtering technique, and tested their method on the same database as in [27,28]. As a classic method of image segmentation, thresholding-based technique was widely applied to segment BUS images. However, determining the optimal threshold value is a critical and difficult problem. Many researchers combined the thresholding-based approach with other methods such as watershed [33], fuzzy clustering [34], active contour model [35], and level set method [36] to obtain improved segmentation results.

Clustering-based

Given a vector of N measurements describing each pixel or group of pixels (i.e., region) in an image, a similarity of the measurement vectors and therefore their clustering in the N-dimensional measurement space imply similarity of the corresponding pixels or pixel groups. Therefore, clustering in measurement space may be an indicator of similarity of image regions and may be used for segmentation. The vector of measurements describes some useful image features and thus is also known as a feature vector. Similarity between image regions or pixels implies clustering (i.e., small separation distance) in the feature space. A comparison from [37] is shown in Fig. 2.

The K-means algorithm is an iterative technique used to partition an image into K clusters. The basic algorithm is: (1) pick K cluster centers, either randomly or based on some heuristic; (2) assign each pixel in the image to the cluster that minimizes the distance between the pixel and the cluster center; (3) recompute the cluster centers by averaging all of the pixels in the cluster; (4) repeat steps (2) and (3) until convergence (i.e., no pixels change clusters). In this case, distance is the squared or absolute difference between a pixel and a cluster center. The difference is typically based on pixel color, intensity, texture, and location, or a weighted combination of these factors. K can be selected manually, randomly, or by a heuristic. This algorithm is guaranteed to converge, but it may not return the optimal solution. The quality of the solution depends on the initial set of clusters and the value of K.

Fuzzy C-means (FCM) clustering is the most widely spread clustering approach for image segmentation because of its robust characteristics for data classification. In 2014, Moon et al. [38] proposed a computer-aided detection (CAD)

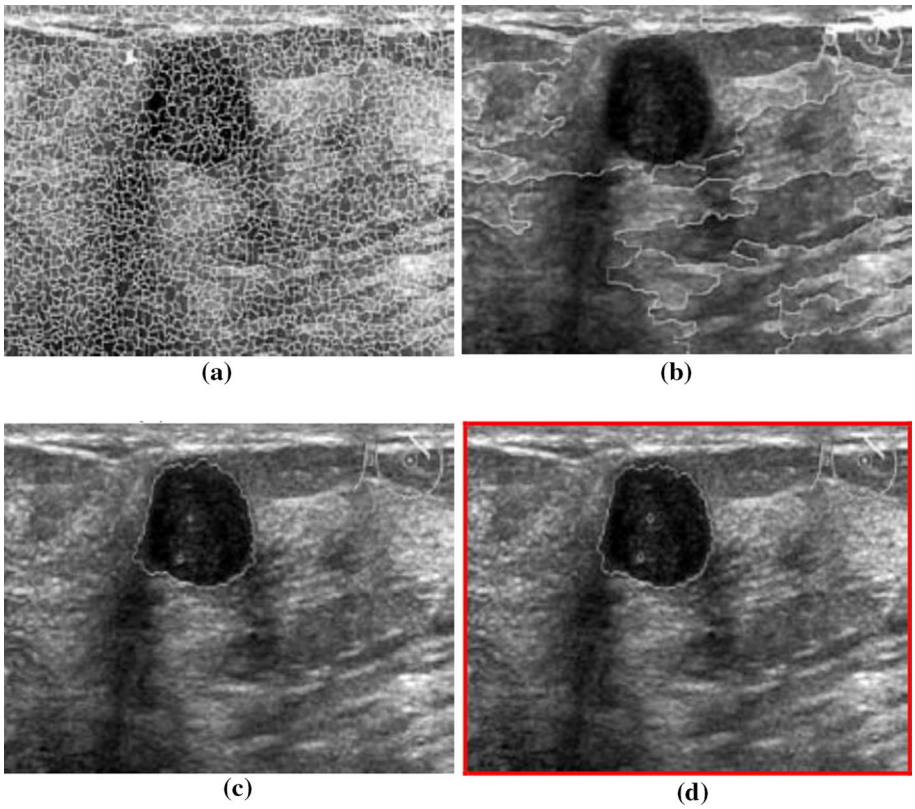

Fig. 2 A comparison of segmentation results using clustering and watershed transform. **a** Watershed transform on original image, **b** marker-controlled watershed transform on original image, **c** clustering on original image, and **d** the clustering-based segmentation method with the histogram equalized probability image [37]

system based on quantitative tissue clustering algorithm to identify potential tumors in automated BUS images, where the hypoechogenic regions, i.e., the tumor candidates, were extracted using the FCM clustering and seven features related to echogenicity and morphology were quantified and used to predict the likelihood of identifying a tumor and filtering out the false positive (FP) regions.

In 2012, Shan et al. [39] developed a novel, effective, and fully automatic method for BUS image segmentation, utilizing a novel phase feature to improve the image quality, and a novel neutrosophic clustering approach to detecting the accurate lesion boundary. First, a ROI was generated to cut off complex background. After speckle reduction, an enhancement algorithm based on phase in max-energy orientation (PMO) was developed to further improve the image quality. The PMO was a newly proposed 2D phase feature obtained by filtering the image in the frequency domain and calculating the phase accumulation in the orientation with maximum energy. Finally, a novel clustering approach called neutrosophic l-means (NLM) was proposed to detect the lesion boundary. It is a generalized clustering method that can be used to solve other clustering problems as well. The NLM was used to segment images with vague boundaries and to deal with uncertainty better. The experimental results showed that the proposed method could generate accurate lesion boundaries even for complicated cases.

Watershed-based

The watershed transformation considers the gradient magnitude of an image as a topographic surface and is a popular image segmentation algorithm for grayscale images [40–45]. Pixels having the highest gradient magnitude intensities correspond to watershed lines, which represent the region boundaries. Water placed on any pixel enclosed by a common watershed line flows downhill to a common local intensity minimum. Pixels draining to a common minimum form a catch basin, which represents a segment. A gray level image may be seen as a topographic relief, where the gray level of a pixel is interpreted as its altitude in the relief. A drop of water falling on a topographic relief flows along a path to finally reach a local minimum. Intuitively, the watershed of a relief corresponds to the limits of the adjacent catchment basins of the drops of water. In image processing, different types of watershed lines may be computed. In graphs, watershed lines may be defined on the nodes, on the edges, or hybrid lines on both nodes and edges. Watersheds may also be defined in the continuous domain. There are also many different algorithms to compute watersheds. Watershed algorithm is used in image processing primarily for segmentation purposes. A segmentation result from [40] is shown in Fig. 3.

Huang and Chen [40,41] once focused on watershed segmentation for BUS images. In 2005, they utilized the watershed transform and active contour model to overcome

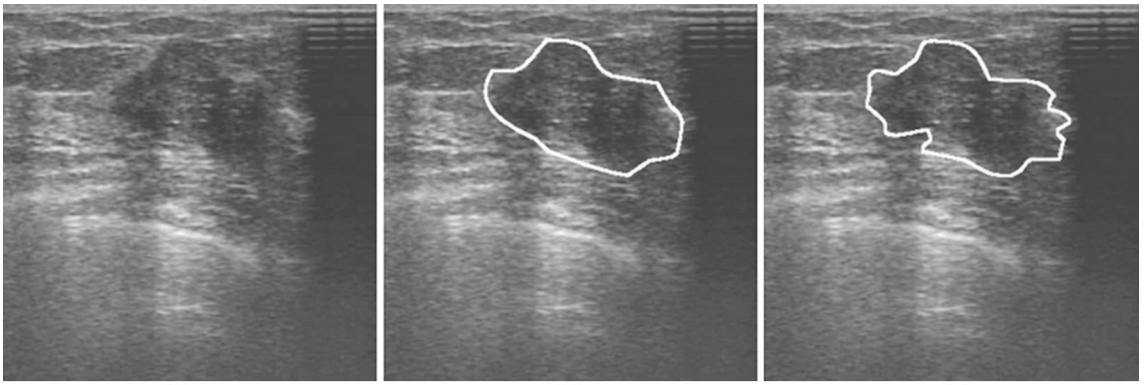

Fig. 3 Watershed transform for BUS segmentation [40]. **a** The original BUS image, **b** manual delineation, and **c** segmentation result

the natural properties of BUS images (i.e., speckle, noise and tissue-related textures) to segment the breast tumor precisely. The watershed transform was performed as the automatic initial contouring procedure to maintain a rough tumor shape and boundary. Next, the active contour model automatically determined the exquisite contour of the tumor. The results of computer simulations revealed that the proposed method always identified similar contours and ROIs as those obtained by manual contouring (by an experienced physician) of the breast tumor in US images.

In 2009, Gomez et al. [42] presented a computerized lesion segmentation technique on BUS images, using morphological filtering, Watershed transform and average radial derivative function. In the next year, they presented another segmentation method for BUS images [43], which consists of three phases as follows. (1) First apply a contrast-enhanced approach, i.e., contrast-limited adaptive histogram equalization. (2) Aiming at removing speckle and enhancing the lesion boundary, an anisotropic diffusion filter, guided by texture descriptors derived from a set of Gabor filters, was applied. To eliminate the distant pixels that do not belong to the tumor, the resulting filtered image was multiplied by a constraint Gaussian function. By doing so, both the segmentation and the marker functions were generated and could be used in the marker-controlled watershed transformation algorithm to create potential lesion boundaries. (3) Finally, to determine the lesion contour, the average radial derivative function was evaluated. The proposed method was tested with 50 BUS images and 60 simulated "US-like" images. In 2011, Zhang et al. [44] employed a novel extended fuzzy watershed method for image segmentation and developed a fully automatic algorithm for BUS image segmentation. The experiments showed that the proposed method could get good results on blurry US images.

The watershed segmentation algorithm is based on the theory of mathematical morphology and the simulation of three-dimensional terrain surface, which belongs to the region-based image segmentation method. The traditional watershed-based segmentation algorithm is sensitive to noise and easy to cause over-segmentation. To this end, efforts have been made in the preprocessing and post-processing of traditional watershed segmentation algorithms.

Graph-based methods

In the last few years, graph-based segmentation has become a research hotspot [46–51] due to the simple structure and solid theories. In this method, the image is modeled as a weighted, undirected graph. Usually a pixel or a group of pixels are associated with nodes and edge weights defining the (dis)similarity between the neighborhood pixels. The graph (image) is then partitioned according to a criterion designed to model "good" clusters. Each partition of the nodes (pixels) output from these algorithms is considered an object segment in the image. Some popular algorithms of this category are graph cuts, normalized cuts, minimum cuts, minimum spanning tree-based segmentation, and segmentation-based object categorization. Typical segmentation results from [47] are shown in Fig. 4.

In 2014, Zhou et al. [46] proposed a new method for semiautomatic tumor segmentation on BUS images using Gaussian filtering, histogram equalization, mean shift, and graph cuts. The only interaction required is to select two diagonal points to determine a ROI in an input image; then, the ROI image is shrunken by a factor of 2 using bicubic interpolation to reduce computation time. Afterward, the shrunken image is smoothed by a Gaussian filter and then contrast-enhanced by the histogram equalization. Next, the enhanced image is filtered by the pyramid mean shift to improve homogeneity. The object and background seeds for graph cuts are automatically generated on the filtered image. Using these seeds, the filtered image is then segmented by graph cuts into a binary image containing the object and background. Finally, the binary image is expanded by a factor of 2 using bicubic interpolation, and the expanded image is processed by morphological opening and closing to refine the tumor

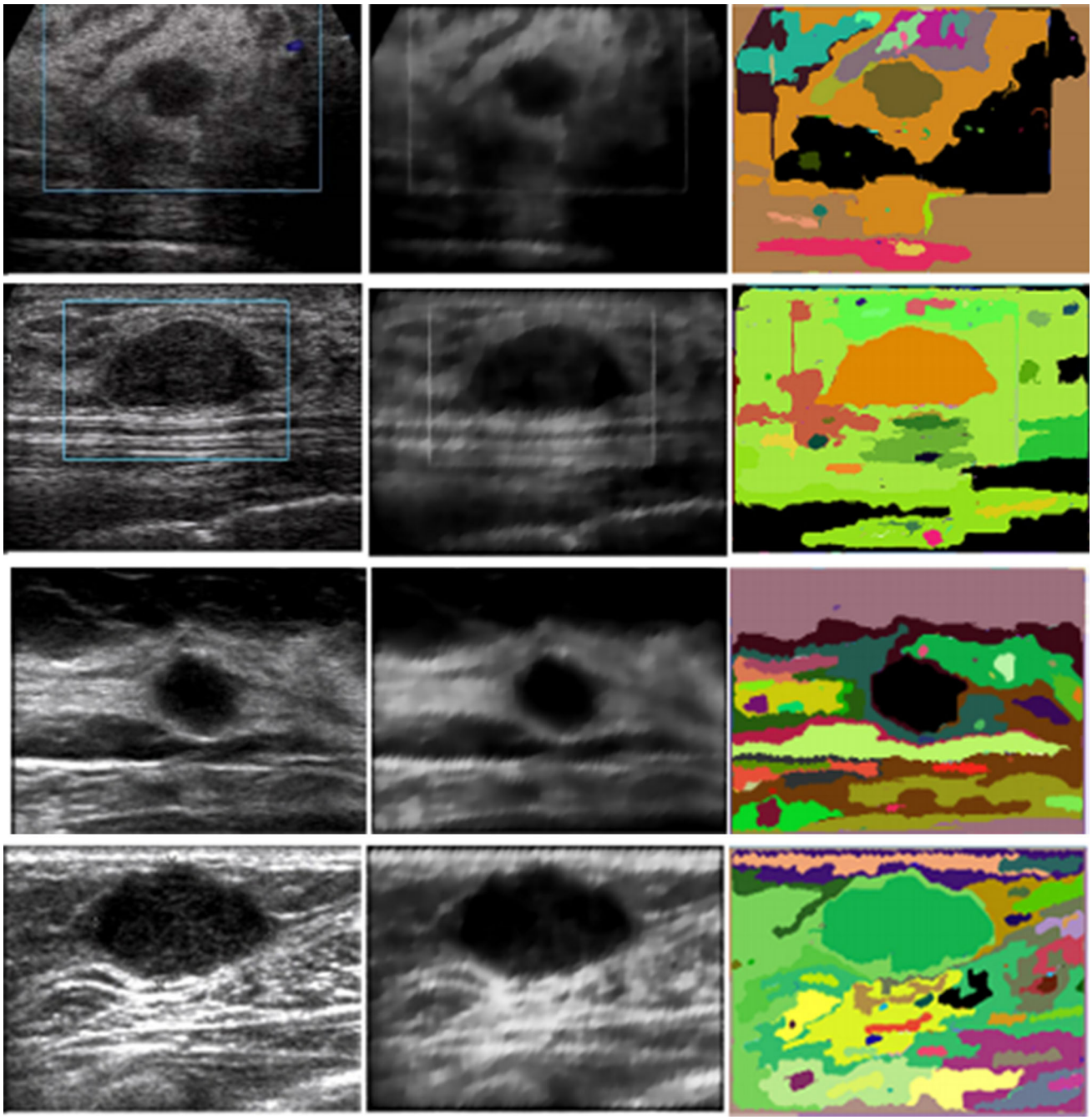

Fig. 4 Segmentation results using graph-based method [47]. The *first column* shows original images, and the *second column* shows filtered images and the *third column* is the segmentation results

contour. The proposed method was tested on a dataset consisting of 38 BUS images with benign tumors and 31 BUS images with malignant tumors from different US scanners. The experimental results indicated that the proposed method may be useful in BUS image segmentation.

After a typical graph-based segmentation method called efficient graph-based image segmentation was proposed and successfully applied to various images in 2004 by Felzenszwalb and Huttenlocher [52], little attention has been paid to applying methods of this kind to US images until 2012, when Huang et al. [47] proposed a method called robust graph-based segmentation method to segment BUS images. In their method, a novel comparison criterion for pairwise subregions, which takes local statistics into account to make their method more robust to noises, was adopted. However, two significant parameters determining the seg-

mentation result were introduced and empirically set, and should be adjusted by repeated test to obtain good segmentation results for different images. Accordingly, Huang et al. [48] proposed a parameter-automatically optimized robust graph-based image segmentation method, which utilizes the particle swarm optimization algorithm to optimize the two key parameters. In addition, Chang et al. [49] took advantage of similar graph theory, and proposed a 3D graph-based segmentation algorithm in 2015.

Among the segmentation algorithms, graph-based segmentation has become a hot spot in the past few years due to its simple structure and solid theory. However, the steps to obtain the TCI and set parameters require user's participation which can lead to significant influence to the following segmentation. To obtain good segmentation results, the operator should be well experienced in examining BUS images and understanding the principle of graph-based segmentation. Consequently, automatic segmentation attracts more and more attention [50], but the computation time would become far away from real-time applications.

Active contour model

The active contour model, more widely known as snake, is another very popular segmentation method for US images [53–59]. It is a framework for delineating an object outline from a possibly noisy 2D image and has been massively used as an edge-based segmentation method. This approach attempts to minimize the energy associated with the initial contour as the sum of the internal and external energies. The active contour model modifies its shape actively and approximates the desired contour. During the deformation process, the force is calculated from the internal energy and external energy. The internal energy derived from the contour model is used to control the shape and regularity of the contour, and the external energy derived from the image feature is used to extract the contour of the desired object.

In 2014, Moraru et al. [57] proposed an efficient image energy function in segmentation based on image features, first-order textural features and four $n \times n$ masks, and developed a method for semiautomatic detection of breast lesion boundaries by combining the snake evolution techniques with the statistical texture information of the image. The experiments indicate that standard deviation, skewness and entropy are the most relevant image features. Meanwhile, Wang et al. [58] presented a multiscale framework for US image segmentation based on speckle reducing anisotropic diffusion (SRAD) and geodesic active contour (GAC). SRAD is an edge-sensitive diffusion tailored for speckled images and was adopted to reduce speckle noise by constructing a multiscale representation for each image where the noise is gradually removed as the scale increases. Then multiscale GACs were applied along the scales in a coarse-to-fine manner to capture the object boundaries progressively. To avoid boundary leakages in low contrast images, traditional GAC model was modified by incorporating the boundary shape similarity between different scales as an additional constraint to guide the contour evolution.

Level set method has been employed to improve the active contour segmentation for US images [53–55]. Huang et al. [53] developed an efficient method for automatically detecting contours of breast tumors in BUS images. First, a sophisticated preprocessing filter reduces the noise, but preserves the shape and contrast of the breast tumors. An adaptive initial contouring method is then performed to obtain an approximate circular contour of the tumor. Finally, the deformation-based level set segmentation automatically extracts the precise contours of breast tumors from BUS images. In 2010, Liu et al. [54] proposed a novel level set-based active contour model for BUS image segmentation. At first, an energy function was formulated according to the differences between the actual and estimated probability densities of the intensities in different regions. The actual probability densities were calculated directly. For calculating the estimated probability densities, the probability density estimation method and background knowledge were utilized. The energy function was formulated with level set approach, and a partial differential equation was derived for finding the minimum of the energy function. For performing numerical computation, the derived partial differential equation was approximated by the central difference and nonreinitialization approach. In 2012, Gao et al. [55] proposed an improved edge-based active contour model method in a variational level set formulation for semiautomatically capturing ultrasonic breast tumor boundaries. However, the methods based on snake-deformation model are used to handle only the ROI, not the entire image. Automatically generating a suitable initial contour is very difficult, and the snake-deformation procedure is very time-consuming. Some segmentation results from [58] are shown in Fig. 5.

The active contour model method has the advantage that ensures the detected edge closed and continuous. Its disadvantage is that the initialization points are needed accurately. In addition, the reasonable energy function is difficult to obtain due to the BUS image quality [54]. The local optimal solution instead of global optimal solution is apt to be obtained. Due to the pseudo edges and noises, it tends to fall into the local minimum solution, or generate oscillation, making it possibly cannot converge to the real edge and therefore decrease the segmentation accuracy.

Markov random field

Because of the presence of artifacts, US image segmentation remains a challenging problem. To solve these problems, Markov random field and maximum a posteriori (MAP)-

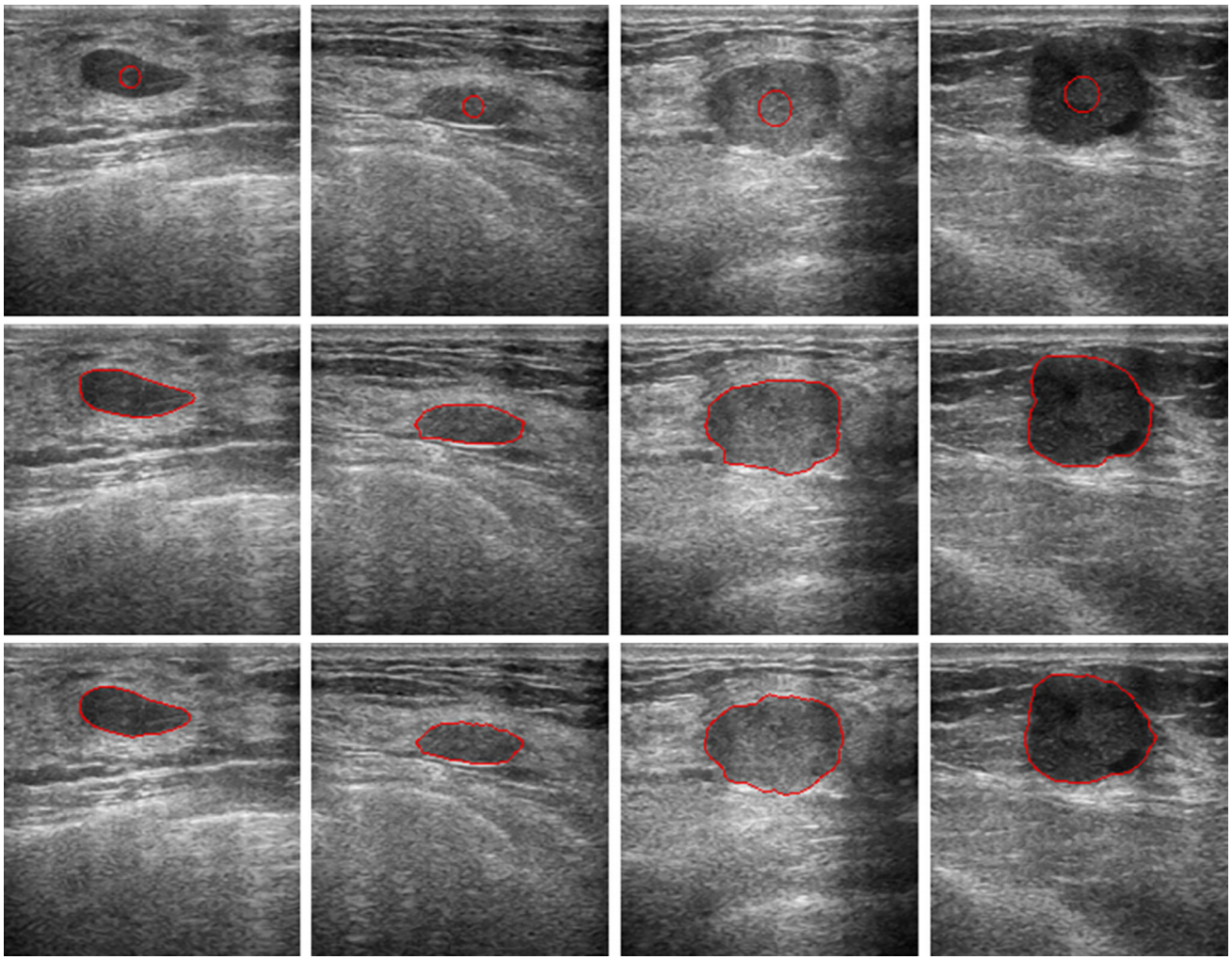

Fig. 5 Active contour model in segmentation of BUS image [58]. *First row* original images overlaid with initial contour; *second row* manual segmentation; *third row* results of the approach based on the active contour model

based methods have been used to estimate a distortion field while identifying regions of similar intensity inhomogeneity. In addition, US image segmentation can be considered as a labeling problem where the solution is to assign a set of labels to pixels, which is a natural representation for MRFs. Markov random field model has already been used for US image segmentation [60–62]. The algorithm alternatively approximates the maximization of the posterior estimation of the class labels, and estimates the class parameters. MRF model deals with the spatial relations between the labels obtained in an iterative segmentation process. The process assigning pixel labels iteratively can be achieved by maximizing either a posteriori estimation or a posterior marginal estimation.

In 2012, Xian et al. [61] proposed a probability model-based method for the accurate and robust segmentation for low quality medical images, which combines the spatial priori knowledge with the frequency constraints under the MAP probability with MRF segmentation framework. The spatial constraints model the global location, the object pose and the appearance, while the objective boundary is constrained in the frequency domain by modeling the phase feature and the zero crossing feature of the wavelet coefficients. The proposed method was tested with a BUS database of 131 cases, and the experimental results showed that this method was accurate and robust in segmenting BUS images. In 2013, Pons et al. [62] exhaustively evaluated different initialization approaches for MRF and MAP using a database of 212 B-mode BUS images and considering the lesion types. They also described the conclusions about the relationship between the lesion types and the segmentation results.

The merit of MRF modeling is that it provides a strong exploitation of the pixel correlations. The segmentation results can be further enhanced by applying MAP segmentation estimation scheme based on the Bayesian learning paradigm. However, its iteration process is complex and time-

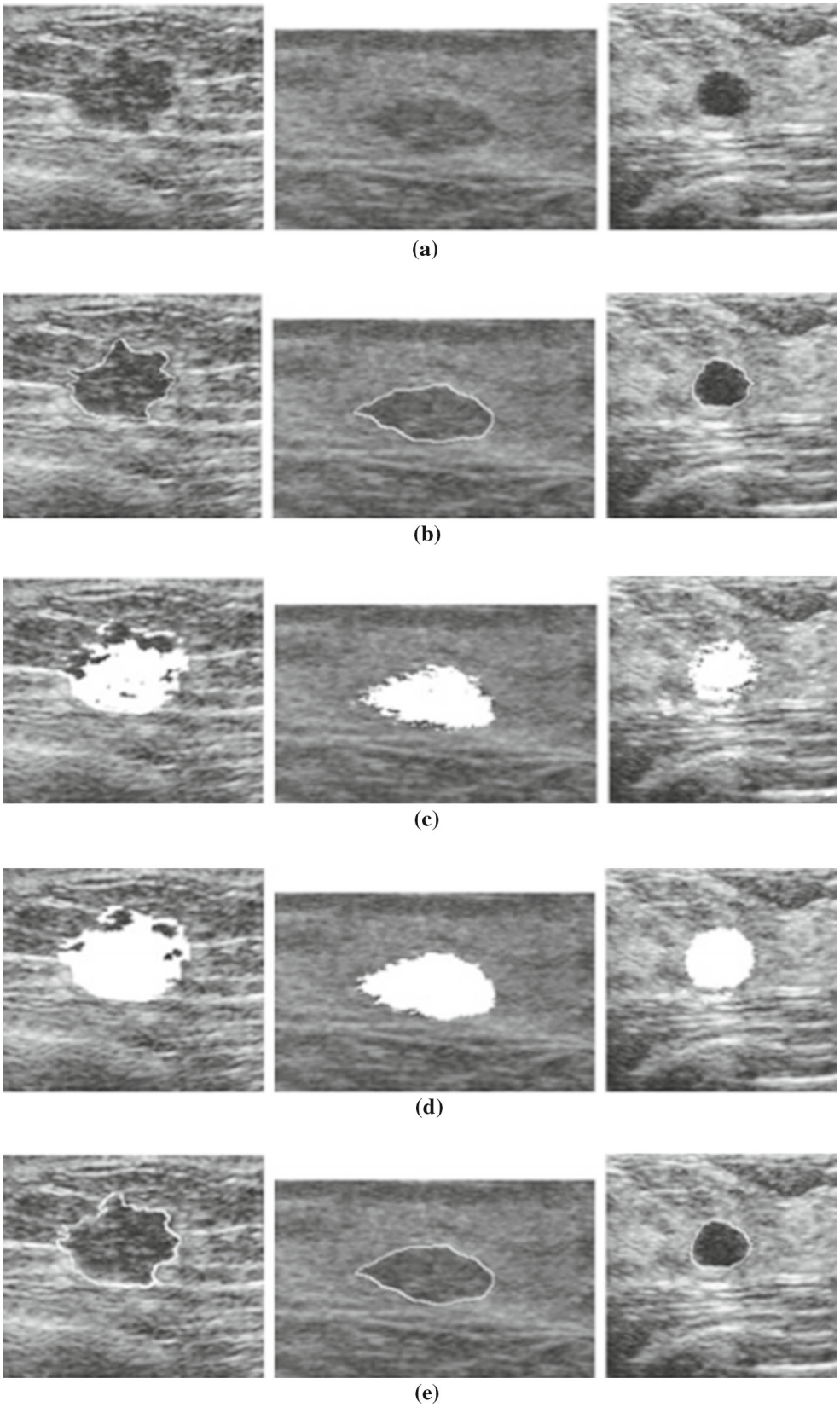

Fig. 6 Markov random field for BUS segmentation [60]. *Left* carcinoma, *center* fibroadenoma, *right* cyst. **a** Original image, **b** true region, **c** ensemble learning-based segmentation without MRF, **d** ensemble learning-based segmentation with MRF, **e** final result using (**d**) as the input

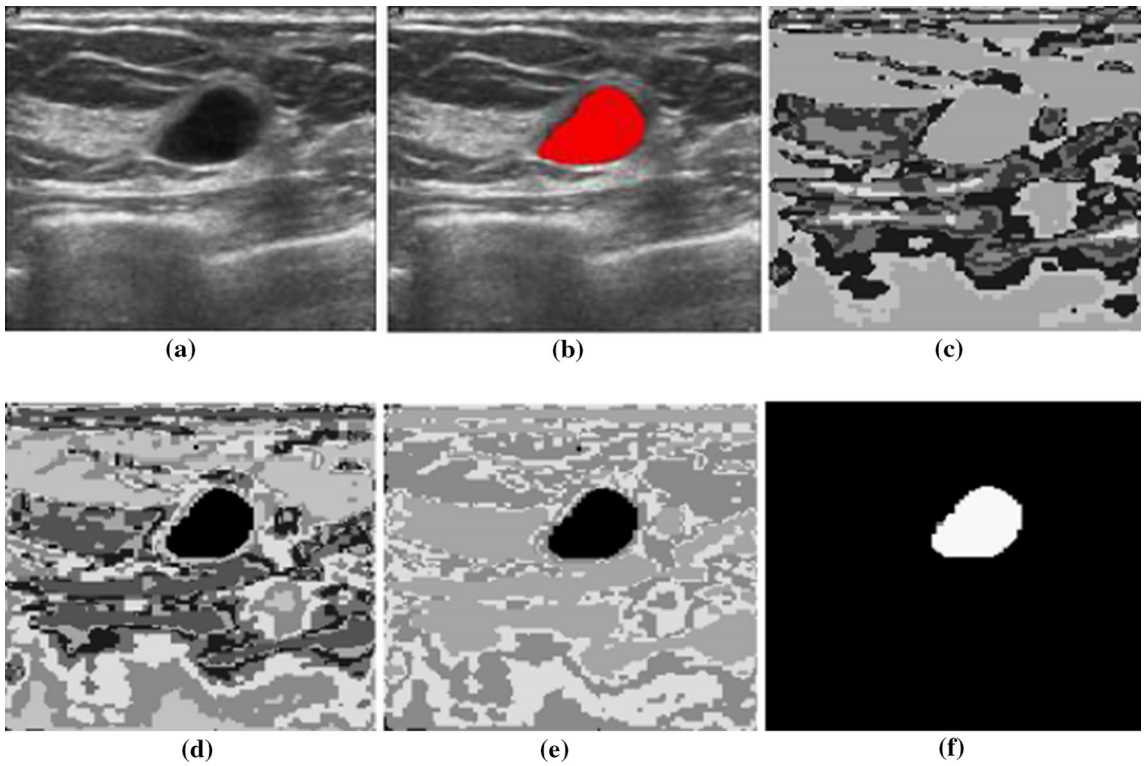

Fig. 7 NN segmentation for BUS [69]. **a** original images, **b** tumor region selected by the physician, **c** segmentation result of the SOM network, **d** segmentation result of the MA-SOM method before merging process, **e** segmentation result of the MA-SOM method after merging process, and **f** tumor region detected by the MA-SOM method

consuming. Some segmentation results from [60] are shown in Fig. 6.

Neural network

Neural network(NN)-based segmentation methods [10,40, 63–70] which transform the segmentation problem into a classification decision based on a set of input features are popular and have proved to be highly accurate [68]. In 1999, Binder et al. [70] investigated the use of artificial neural network for image segmentation and spatial temporal contour linking for the detection of endocardial contours on echocardiographic images. Although not a recent research, it is a good illustration of the application of the neural network learning to US image segmentation. It is also one of the few US image segmentation methods that have been explicitly tested on a reasonable number of clinical images with varied quality.

In Re. F5, a simplified pulse coupled neural network (PCNN) model was proposed and the fuzzy mutual information (FMI) was improved as the optimization criterion for the simplified PCNN. Then the simplified PCNN and improved FMI (IFMI)-based segmentation algorithm was proposed and applied to the segmentation of breast tumor in BUS images. In 2011, Jiao and Wang [65] proposed a novel segmentation method for the BUS image by using a two-stage strategy: the ROI generation and segmentation. In the same year, Othman and Tizhoosh [66] proposed two different approaches to segmenting the BUS image based on NN. In the first approach, the scale invariant feature transform (SIFT) was used to calculate a set of descriptors for a set of points inside the image, then these descriptors were used to train a supervised NN. In the second approach, the SIFT was used to detect a set of key points inside the image, and texture features were then extracted from the region around each point to train the NN. In 2014, Torbati et al. [69] proposed a new NN-based method for medical image segmentation. Their method was tested on BUS images, X-ray computerized tomography (CT) images, and magnetic resonance (MR) head images. The segmentation results of BUS images demonstrated that there was a significant correlation between the tumor region selected by a physician and the tumor region segmented by their proposed method. A segmentation result from [69] is shown in Fig. 7.

As a classic supervised learning method, NN-based segmentation method which transforms the segmentation problem into a classification decision has been proved highly accurately [68]. It only cares about which category sample points belong to, ignoring the spatial distribution of sample set. Thus, it could be expected that using deep learning model

may be a topic for segmentation of BUS images. However, the NN models are relatively time-consuming [10,67] during the training, which is a certain limitation.

Performance evaluation of segmentation methods

To quantitatively measure the experiment results, some criteria are adopted in the research. The averaged radial error (ARE) [47] was used for the evaluation of segmentation performance by measuring the average radial error of a segmented contour with respect to the real contour delineated by an expert radiologist. Figures 8 and 9 show two cases in each of which the difference between the computed contour using a segmentation method and manually sketched contour that often is regarded as the actual boundary. As shown in Fig. 8, the ARE is defined as:

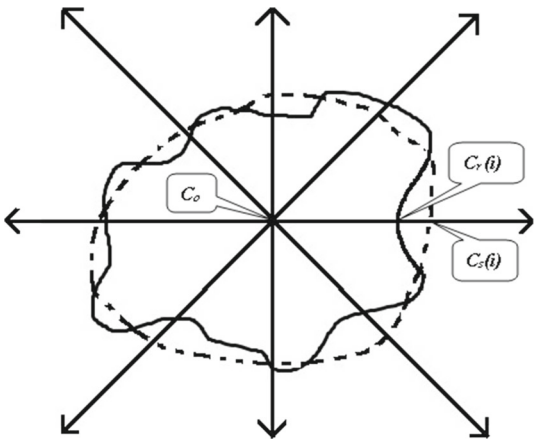

Fig. 8 C_r is the manually sketched contours and C_s is contours generated by the computer system

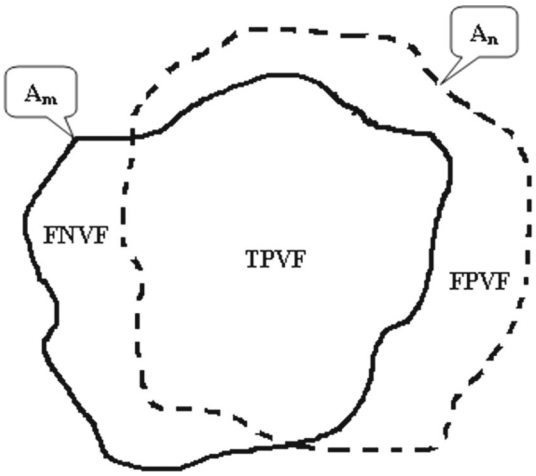

Fig. 9 A_m is the region covered by manually sketched contours and A_n is the region covered by contours generated by the computer system

$$\mathrm{ARE}(n) = \frac{1}{n}\sum_{i=0}^{n-1}\frac{|C_s(i) - C_r(i)|}{|C_r(i) - C_o|} \times 100\% \tag{2}$$

True positive (TP), false positive (FP), false negative(FN), and similarity(SI) are also often used in the evaluation of the performance of segmentation methods. TP, one of the most commonly used evaluation metrics, indicates the total fraction of tissue in the "true" tumor region with which the segmented region overlaps. FP denotes the amount of tissue falsely identified by the segmentation method as a fraction of the total amount of tissue in the "true" tumor region. FN denotes the fraction of tissue defined in the "true" tumor region that is missed by the segmentation method and SI (some articles are also called it *overlap* or *Jaccard index*) measures the overlap ratio. Accordingly, smaller ARE, FP and FN, and larger TP and SI indicate better segmentation performance. As shown in Fig. 9, the four evaluation metrics are defined as:

$$\mathrm{TP} = \text{true positive} = \frac{A_m \cap A_n}{A_m} \tag{3}$$

$$\mathrm{FP} = \text{false positive} = \frac{A_n - A_m \cap A_n}{A_m} \tag{4}$$

$$\mathrm{SI} = \text{similarity} = \frac{A_m \cap A_n}{A_m \cup A_n} \tag{5}$$

$$\mathrm{FP} = \text{false positive} = \frac{A_m - A_m \cap A_n}{A_m} \tag{6}$$

In Ref. [40], the precision ratio (PR) and the match rate (MR) are used to evaluate the performance numerically. The PR denotes the precision ratio between the manually determined contours and the automatically detected contours and the MR denotes the match rate. The PR and MR are defined as:

$$\begin{aligned}\mathrm{PR} = \text{precision ratio} &= \frac{N_{\mathrm{diff}}}{N_m} \times 100\% \\ &= \frac{(A_m - A_m \cap A_n) \cup (A_n - A_m \cap A_n)}{A_m}\end{aligned} \tag{7}$$

$$\mathrm{MR} = \text{match rate} = \left(1 - \frac{|\mathrm{Area}_m - \mathrm{Area}_n|}{\mathrm{Area}_m}\right) \times 100\% \tag{8}$$

where N_{diff} is the number of pixels that differ between the manually determined contour and the automatically determined contour, and N_m is the number of pixels in the manual contour. Area_m and Area_n mean the superficial measurement of the region A_m and A_n.

In Ref. [43], the normalized residual value (NRV) and proportional distance (PD) are introduced to evaluate the performance. The NRV and PD are defined as:

Table 1 Comparison of different techniques

Techniques	References	Dataset size	Accuracy	Time (s)	Auto.
Thresholding-based	Horsch et al. [27]	400	Overlap = 94%	–	Semi.
	Yap et al. [31]	360	TP = 86%	–	Auto.
Clustering-based	Shan et al. [39]	122	TP = 92.4% FP = 7.2% SI = 86.3%	–	Auto.
Watershed-based	Huang et al. [40]	60	PR = 81.7% MR = 94.7%	–	Auto.
	Gomez et al. [43]	50	SI = 86.0% NRV = 0.15 PD = 6.28%	25.0	Semi.
Graph-based	Huang et al. [47]	20	ARE = 9.1 TP = 87.5% FP = 2.5%	9.3	Semi.
	Zhou et al. [46]	69	TP = 93.1% FP = 9.7% SI = 89.6%	0.49 ± 0.36	Semi.
ACM	Liu et al. [54]	79	TP = 93.9% FP = 7.0% SI = 88.1%	60.4	Semi.
	Gao et al. [55]	20	TP = 90.8% FP = 4.2% SI = 86.3%	–	Semi.
MRF	Takemura et al. [60]	400	SI = 93.4%	280.0	Auto.
	Xian et al. [61]	131	TP = 90.12% P = 7.62% SI = 84.10%	–	Auto.
NN	Shan et al. [67]	120	TP = 92.8% FP = 12.0% SI = 83.1%	9.5	Auto.

Auto. automatic, *Semi.* semiautomatic

$$\text{NRV} = \text{normalized residual value} = \frac{A_m \oplus A_n}{A_m} = \frac{(A_m - A_m \cap A_n) \cup (A_n - A_m \cap A_n)}{A_m} \quad (9)$$

$$\text{PD} = \text{proportional distance} = \frac{\frac{\sum_{X_i \in C_r} d(X_i, C_S)}{|C_r|} + \frac{\sum_{X_i \in C_c} d(X_i, C_r)}{|C_S|}}{2\sqrt{\frac{A_m}{\pi}}} \times 100 \quad (10)$$

where (X_i, C) is the geometrical distance from a point X_i to the contour C, and $|C|$ is the number of points in C.

Performance overview

In this paper, we have reviewed the literature on the segmentation of BUS images according to the techniques adopted, especially over the past 10 years. By dividing into seven classes (i.e., thresholding-based, clustering-based, watershed-based, graph-based, ACM, MRF, and NN), we have introduced corresponding techniques and representative papers accordingly. Table 1 summarizes the performances of a number of often used BUS segmentation algorithms, making the comparison more convenient.

In Table 1, we can see many techniques and papers on BUS image segmentation, especially over the past 10 years. All these techniques have their own pros and cons. As the simplest method of image segmentation, thresholding-based technique was widely applied to segmenting BUS images. However, thresholding-based methods do not perform well for the image with a unimodal histogram. Clustering is a classification technique, and its performance heavily relies on the similarity measurement. As a classical clustering method, the performance of k-means depends on the initial set of clusters and the value of k. The watershed transformation considers the gradient magnitude of an image as a topographic surface, and its performance is various for different types of computed watershed lines. In graph-based methods, the image is modeled as a weighted, undirected graph, and the performance also relies on the similarity measurement. The ACM is a very popular segmentation method, but automatically generating a suitable initial contour is difficult, and the deformation procedure is time-consuming [54]. The MRF

modeling provides a strong exploitation of the pixel correlations, and the segmentation result can be further enhanced by applying MAP. However, its iteration process is very complex and time-consuming [60]. The NN-based methods have proved to be highly accurate [68]. However, they are relatively time-consuming as well [10,67].

Discussion and conclusions

According to Table 1, we can see that different methods were tested on different datasets, and different measurements were calculated to measure the overall performance. This makes it difficult to compare and evaluate different algorithms. Therefore, it is an urgent task to build a benchmark database of BUS images accessible to the public to support the comparison and evaluation of different algorithms, and standard measurements should be selected as well.

However, BUS image segmentation is still an open and challenging problem due to various US artifacts introduced in the process of imaging, including high speckle noise, low contrast, blurry boundaries, low signal-to-noise ratio and intensity inhomogeneity. Besides, the appearances of benign and malignant tumors are different in clinical BUS images, and the operations of radiologists are also quite different, which both contribute to the difficulty of BUS image segmentation. The quality of BUS image also depends on different ultrasonic devices.

In addition, posterior acoustic shadowing which appears as a dark vertical patch region posterior to the lesion often obfuscates lesion margins, making it difficult to accurately determine lesion shape. It is similar in the intensity characteristic between lesion and posterior acoustic shadowing region, leading to difficulty in BUS images segmentation and subsequent analysis [71]. The problem of posterior acoustic shadowing in BUS image has been overlooked in many BUS CAD systems. Drukker et al. [72] investigated the skewness values within manually defined ROI to analyze posterior acoustic shadowing in BUS image. Anant et al. [71] proposed a method which used nonlinear dimensionality reduction and adaboost method to discriminate between lesions and posterior acoustic shadowing by combining the different image features. Nevertheless, it remains a challenging issue and needs more attentions and efforts in academic and engineering fields.

BUS image segmentation remains an open problem. With advancement of image processing technology, some new techniques [73,74] have been introduced into traditional techniques to achieve better segmentation results. In the process of improving the segmentation accuracy, proposing automatic and real-time segmentation methods will be a main trend in this field [39,53,67]. In addition, with the development of 3D US imaging and the speedily increasing use of 3D imaging modalities, attention to 3D US segmentation methods is gradually increased in the coming years [63].

To the best of our knowledge, this is the first comprehensive review of the approaches developed for segmentation of BUS images. With most techniques involved, this paper will be useful and helpful for researchers in segmentation of US images (e.g., choosing investigation direction, comparing different techniques and improving existing methods), and for breast cancer CAD developers in choosing segmentation methods according to their own requirements.

Funding This work was partially funded by National Natural Science Foundation of China (Nos. 61271314, 61372007, 61401286, and 61571193) and Guangdong Provincial Science and Technology Program—International Collaborative Projects (No. 2014A050503020).

Compliance with ethical standards

Conflict of interest The authors declare that they have no conflict of interest.

Informed consent For this type of study, formal consent is not required, and this article does not contain patient data.

Human and animal rights This article does not contain any studies with human participants or animals performed by any of the authors.

References

1. Cheng HD, Cai X, Chen X, Hu L, Lou X (2003) Computer-aided detection and classification of microcalcifications in mammograms: a survey. Pattern Recognit 36(12):2967–2991
2. Lee CH (2002) Screening mammography: proven benefit, continued controversy. Radiol Clin N Am 40(3):395–407
3. Cheng HD, Shi XJ, Min R, Hu LM, Cai XP, Du HN (2006) Approaches for automated detection and classification of masses in mammograms. Pattern Recognit 39(4):646–668
4. Jesneck JL, Lo JY, Baker JA (2007) Breast mass lesions: computer-aided diagnosis models with mammographic and sonographic descriptors. Radiology 244(2):390–398
5. Bird RE, Wallace TW, Yankaskas BC (1992) Analysis of cancers missed at screening mammography. Radiology 184(3):613–617
6. Kerlikowske K, Carney PA, Geller B, Mandelson MT, Taplin SH, Malvin K, Ballard-Barbash R (2000) Performance of screening mammography among women with and without a first-degree relative with breast cancer. Ann Intern Med 133(11):855–863
7. Giger ML (2002) Computer-aided diagnosis in radiology. Acad Radiol 9(1):1–3
8. Sahiner B, Chan HP, Roubidoux MA, Hadjiiski LM, Helvie MA, Paramagul C, Blane C (2007) Malignant and benign breast masses on 3D US volumetric images: effect of computer-aided diagnosis on radiologist accuracy 1. Radiology 242(3):716–724
9. Chen CM, Chou YH, Han KC, Hung GS, Tiu CM, Chiou HJ, Chiou SY (2003) Breast lesions on sonograms: computer-aided diagnosis with nearly setting-independent features and artificial neural networks 1. Radiology 226(2):504–514
10. Drukker K, Giger ML, Horsch K, Kupinski MA, Vyborny CJ, Mendelson EB (2002) Computerized lesion detection on breast ultrasound. Med Phys 29(7):1438–1446
11. Costantini M, Belli P, Lombardi R, Franceschini G, Mulè A, Bonomo L (2006) Characterization of solid breast masses use of

the sonographic breast imaging reporting and data system lexicon. J Ultrasound Med 25(5):649–659
12. Anderson BO, Shyyan R, Eniu A, Smith RA, Yip CH, Bese NS, Carlson RW (2006) Breast cancer in limited-resource countries: an overview of the breast health global initiative 2005 guidelines. Breast J 12(s1):S3–S15
13. Shankar PM, Piccoli CW, Reid JM, Forsberg F, Goldberg BB (2005) Application of the compound probability density function for characterization of breast masses in ultrasound B scans. Phys Med Biol 50(10):2241–2248
14. Taylor KJ, Merritt C, Piccoli C, Schmidt R, Rouse G, Fornage B, Mendelson E (2002) Ultrasound as a complement to mammography and breast examination to characterize breast masses. Ultrasound Med Biol 28(1):19–26
15. Zhi H, Ou B, Luo BM, Feng X, Wen YL, Yang HY (2007) Comparison of ultrasound elastography, mammography, and sonography in the diagnosis of solid breast lesions. J Ultrasound Med 26(6):807–815
16. Drukker K, Giger M, Meinel LA, Starkey A, Janardanan J, Abe H (2013) Quantitative ultrasound image analysis of axillary lymph node status in breast cancer patients. Int J Comput Assist Radiol Surg 8(6):895–903
17. Chang RF, Wu WJ, Moon WK, Chen DR (2003) Improvement in breast tumor discrimination by support vector machines and speckle-emphasis texture analysis. Ultrasound Med Biol 29(5):679–686
18. André MP, Galperin M, Olson LK, Richman K, Payrovi S, Phan P (2002) Improving the accuracy of diagnostic breast ultrasound. In: Maev RG (ed) Acoustical imaging. Springer, US, pp 453–460
19. Huang YL, Chen DR, Liu YK (2004, October) Breast cancer diagnosis using image retrieval for different ultrasonic systems. In: 2004 International conference on image processing, 2004. ICIP'04, vol 5. IEEE, pp 2957–2960
20. Ikedo Y, Morita T, Fukuoka D, Hara T, Lee G, Fujita H, Endo T (2009) Automated analysis of breast parenchymal patterns in whole breast ultrasound images: preliminary experience. Int J Comput Assist Radiol Surg 4(3):299–306
21. Yu-Len H, Yu-Ru J, Jia-Jia S, Dar-Ren C, Kyung MW (2007) Computer-aided diagnosis with morphological features for breast lesion on sonograms. Int J Comput Assist Radiol Surg 2(Suppl. 1):S344–S346
22. Noble JA, Boukerroui D (2006) Ultrasound image segmentation: a survey. IEEE Trans Med Imaging 25(8):987–1010
23. Wells PNT, Halliwell M (1981) Speckle in ultrasonic imaging. Ultrasonics 19(5):225–229
24. Xiao G, Brady M, Noble JA, Zhang Y (2002) Segmentation of ultrasound B-mode images with intensity inhomogeneity correction. IEEE Trans Med Imaging 21(1):48–57
25. Cheng HD, Shan J, Ju W, Guo Y, Zhang L (2010) Automated breast cancer detection and classification using ultrasound images: a survey. Pattern Recognit 43(1):299–317
26. Jalalian A, Mashohor SB, Mahmud HR, Saripan MIB, Ramli ARB, Karasfi B (2013) Computer-aided detection/diagnosis of breast cancer in mammography and ultrasound: a review. Clin Imaging 37(3):420–426
27. Horsch K, Giger ML, Venta LA, Vyborny CJ (2001) Automatic segmentation of breast lesions on ultrasound. Med Phys 28(8):1652–1659
28. Horsch K, Giger ML, Venta LA, Vyborny CJ (2002) Computerized diagnosis of breast lesions on ultrasound. Med Phys 29(2):157–164
29. Xian M, Zhang Y, Cheng HD (2015) Fully automatic segmentation of breast ultrasound images based on breast characteristics in space and frequency domains. Pattern Recognit 48(2):485–497
30. Horsch K, Giger ML, Vyborny CJ, Venta LA (2004) Performance of computer-aided diagnosis in the interpretation of lesions on breast sonography. Acad Radiol 11(3):272–280
31. Yap MH, Edirisinghe EA, Bez HE (2007, March) Fully automatic lesion boundary detection in ultrasound breast images. In: Pluim JPW, Reinhardt JM (eds) International Society for Optics and Photonics. Medical Imaging, San Diego, CA, pp 65123I-1–65123I-8
32. Rodrigues PS, Giraldi GA (2011) Improving the non-extensive medical image segmentation based on Tsallis entropy. Pattern Anal Appl 14(4):369–379
33. Mustaqeem A, Javed A, Fatima T (2012) An efficient brain tumor detection algorithm using watershed & thresholding based segmentation. Int J Image Graph Signal Process 4(10):34
34. Filipczuk P, Kowal M, Obuchowicz A (2011) Fuzzy clustering and adaptive thresholding based segmentation method for breast cancer diagnosis. In: Burduk R, Kurzyński M, Woźniak M, Żołnierek A (eds) Computer recognition systems, vol 4. Springer, Berlin, pp 613–622
35. Altarawneh NM, Luo S, Regan B, Sun C, Jia F (2014) Global threshold and region-based active contour model for accurate image segmentation. Signal Image Process 5(3):1
36. Dirami A, Hammouche K, Diaf M, Siarry P (2013) Fast multilevel thresholding for image segmentation through a multiphase level set method. Signal Process 93(1):139–153
37. Kekre HB, Shrinath P (2013) Tumour delineation using statistical properties of the breast US images and vector quantization based clustering algorithms. Int J Image Graph Signal Process 5(11):1–12
38. Moon WK, Lo CM, Chen RT, Shen YW, Chang JM, Huang CS, Chang RF (2014) Tumor detection in automated breast ultrasound images using quantitative tissue clustering. Med Phys 41(4):042901
39. Shan J, Cheng HD, Wang Y (2012) A novel segmentation method for breast ultrasound images based on neutrosophic l-means clustering. Med Phys 39(9):5669–5682
40. Huang YL, Chen DR (2004) Watershed segmentation for breast tumor in 2-D sonography. Ultrasound Med Biol 30(5):625–632
41. Huang YL, Chen DR (2006) Automatic contouring for breast tumors in 2-D sonography. In: 2005 27th annual conference IEEE engineering in medicine and biology. IEEE, pp 3225–3228
42. Gomez W, Leija L, Pereira WCA, Infantosi AFC (2009, March) Morphological operators on the segmentation of breast ultrasound images. In: 2009 Pan American Health Care Exchanges. IEEE, pp 67–71
43. Gomez W, Leija L, Alvarenga AV, Infantosi AFC, Pereira WCA (2010) Computerized lesion segmentation of breast ultrasound based on marker-controlled watershed transformation. Med Phys 37(1):82–95
44. Zhang L, Zhang M (2011) A fully automatic image segmentation using an extended fuzzy set. In: Yu Y, Yu Z, Zhao J (eds) Computer science for environmental engineering and ecoinformatics. Springer, Berlin, pp 412–417
45. Lo CM, Chen RT, Chang YC, Yang YW, Hung MJ, Huang CS, Chang RF (2014) Multi-dimensional tumor detection in automated whole breast ultrasound using topographic watershed. IEEE Trans Med Imaging 33(7):1503–1511
46. Zhou Z, Wu W, Wu S, Tsui PH, Lin CC, Zhang L, Wang T (2014) Semi-automatic breast ultrasound image segmentation based on mean shift and graph cuts. Ultrason Imaging 0161734614524735:1–21
47. Huang QH, Lee SY, Liu LZ, Lu MH, Jin LW, Li AH (2012) A robust graph-based segmentation method for breast tumors in ultrasound images. Ultrasonics 52(2):266–275
48. Huang Q, Bai X, Li Y, Jin L, Li X (2014) Optimized graph-based segmentation for ultrasound images. Neurocomputing 129:216–224
49. Chang H, Chen Z, Huang Q, Shi J, Li X (2015) Graph-based learning for segmentation of 3D ultrasound images. Neurocomputing 151:632–644

50. Huang Q, Yang F, Liu L, Li X (2015) Automatic segmentation of breast lesions for interaction in ultrasonic computer-aided diagnosis. Inf Sci 314:293–310
51. Eapena MM, Ancelita MSJA, Geetha G (2015) Segmentation of tumors from ultrasound images with PAORGB. Procedia Comput Sci 50:663–668
52. Felzenszwalb PF, Huttenlocher DP (2004) Efficient graph-based image segmentation. Int J Comput Vis 59(2):167–181
53. Huang YL, Jiang YR, Chen DR, Moon WK (2007) Level set contouring for breast tumor in sonography. J Digit Imaging 20(3):238–247
54. Liu B, Cheng HD, Huang J, Tian J, Tang X, Liu J (2010) Probability density difference-based active contour for ultrasound image segmentation. Pattern Recognit 43(6):2028–2042
55. Gao L, Liu X, Chen W (2012) Phase-and GVF-based level set segmentation of ultrasonic breast tumors. J Appl Math 2012:1–22
56. Rodtook A, Makhanov SS (2013) Multi-feature gradient vector flow snakes for adaptive segmentation of the ultrasound images of breast cancer. J Vis Commun Image Represent 24(8):1414–1430
57. Moraru L, Moldovanu S, Biswas A (2014) Optimization of breast lesion segmentation in texture feature space approach. Med Eng Phys 36(1):129–135
58. Wang W, Zhu L, Qin J, Chui YP, Li BN, Heng PA (2014) Multiscale geodesic active contours for ultrasound image segmentation using speckle reducing anisotropic diffusion. Opt Lasers Eng 54:105–116
59. Rodrigues R, Braz R, Pereira M, Moutinho J, Pinheiro AM (2015) A two-step segmentation method for breast ultrasound masses based on multi-resolution analysis. Ultrasound Med Biol 41(6):1737–1748
60. Takemura A, Shimizu A, Hamamoto K (2010) A cost-sensitive extension of AdaBoost with markov random field priors for automated segmentation of breast tumors in ultrasonic images. Int J Comput Assist Radiol Surg 5(5):537–547
61. Xian M, Huang J, Zhang Y, Tang X (2012, September) Multiple-domain knowledge based MRF model for tumor segmentation in breast ultrasound images. In 2012 19th IEEE international conference on image processing. IEEE, pp 2021–2024
62. Pons G, Martí J, Martí R, Ganau S, Vilanova JC, Noble JA (2013) Evaluating lesion segmentation on breast sonography as related to lesion type. J Ultrasound Med 32(9):1659–1670
63. Huang SF, Chen YC, Moon WK (2008, May) Neural network analysis applied to tumor segmentation on 3D breast ultrasound images. In: 2008 5th IEEE international symposium on biomedical imaging: from nano to macro. IEEE, pp 1303–1306
64. Shi J, Xiao Z, Zhou S (2010) Automatic segmentation of breast tumor in ultrasound image with simplified PCNN and improved fuzzy mutual information. In: Visual communications and image processing 2010. International Society for Optics and Photonics, pp 77441P–77441P-8
65. Jiao J, Wang Y (2011) Automatic boundary detection in breast ultrasound images based on improved pulse coupled neural network and active contour model. In: 2011 5th International conference on bioinformatics and biomedical engineering (iCBBE). IEEE, pp 1–4
66. Othman AA, Tizhoosh HR (2011) Segmentation of breast ultrasound images using neural networks. In: Iliadis L, Jayne C (eds) Engineering applications of neural networks. Springer, Berlin, pp 260–269
67. Shan J, Cheng HD, Wang Y (2012) Completely automated segmentation approach for breast ultrasound images using multiple-domain features. Ultrasound Med Biol 38(2):262–275
68. Marcomini KD, Schiabel H, Carneiro AAO (2013, February) Quantitative evaluation of automatic methods for lesions detection in breast ultrasound images. In: Novak CL, Aylward S (eds) SPIE medical imaging. International Society for Optics and Photonics, Orlando, pp 867027–867027-7
69. Torbati N, Ayatollahi A, Kermani A (2014) An efficient neural network based method for medical image segmentation. Comput Biol Med 44:76–87
70. Binder T, Süssner M, Moertl D, Strohmer T, Baumgartner H, Maurer G, Porenta G (1999) Artificial neural networks and spatial temporal contour linking for automated endocardial contour detection on echocardiograms: a novel approach to determine left ventricular contractile function. Ultrasound Med Biol 25(7):1069–1076
71. Madabhushi A, Yang P, Rosen M, Weinstein S (2006) Distinguishing lesions from posterior acoustic shadowing in breast ultrasound via non-linear dimensionality reduction. In: 28th Annual international conference of the IEEE engineering in medicine and biology society, 2006. EMBS'06. IEEE, pp 3070–3073
72. Drukker K, Giger ML, Mendelson EB (2003) Computerized analysis of shadowing on breast ultrasound for improved lesion detection. Med Phys 30(7):1833–1842
73. Kim H, Kim H, Hong H (2015) Chest wall segmentation in automated 3D breast ultrasound using rib shadow enhancement and multi-plane cumulative probability enhanced map. In: Hadjiiski LM, Tourassi GD (eds) SPIE medical imaging. International Society for Optics and Photonics, Orlando, pp 941423-1–941423-8
74. Massich J, Lemaître G, Martí J, Mériaudeau F (2015) Breast ultrasound image segmentation: an optimization approach based on super-pixels and high-level descriptors. In: The international conference on quality control by artificial vision 2015. International Society for Optics and Photonics, pp 95340C–95340C-8